Microwave-pulse synthesis of tunable 2D porous nickel-enriched $LaMn_xNi_{1-x}O_3$ solid solution for efficient electrocatalytic urea oxidation

Zhiao Wu, ‡[a] Jinglin Xian, ‡[a] Jiao Dai, ‡[a] Guangyu Fang, [a] Miao Fan, [a] Haoran Tian, [a] Jiayue Guo, [a] Huiyu Jiang, [a] Weilin Xu, [a] and Jun Wan *[a]

Supplementary materials:
1. Fig. S1 to S19
2. Table S1 to S2

1. Fig. S1 to S19

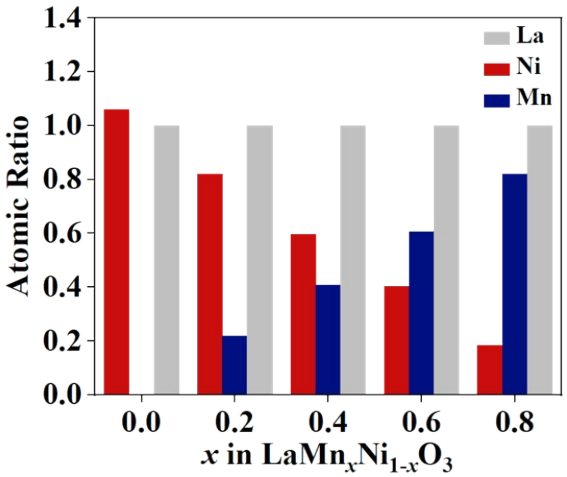

Fig. S1 Average atomic ratio of La, Ni and Mn in $LaMn_xNi_{1-x}O_3$ (x=0, 0.2, 0.4, 0.6, 0.8) samples.

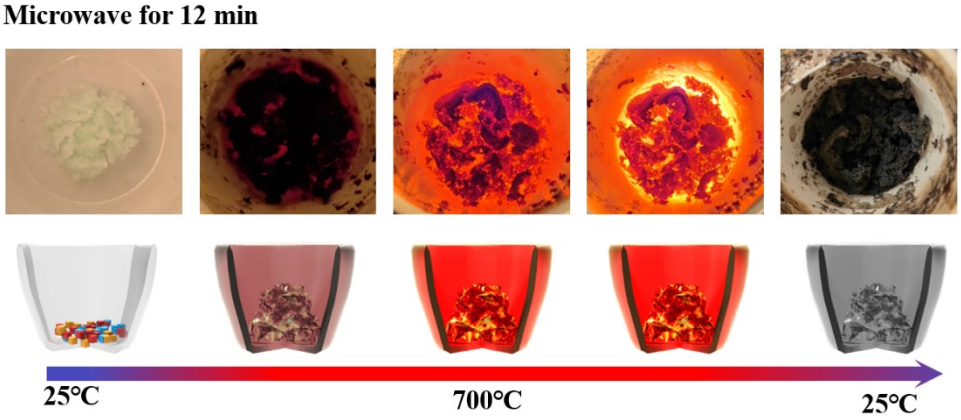

Fig. S2 Physical image of sample reaction changes.

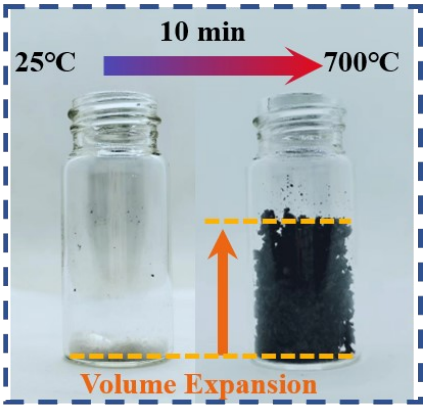

Fig. S3 Physical-optical photographs before and after the reaction.

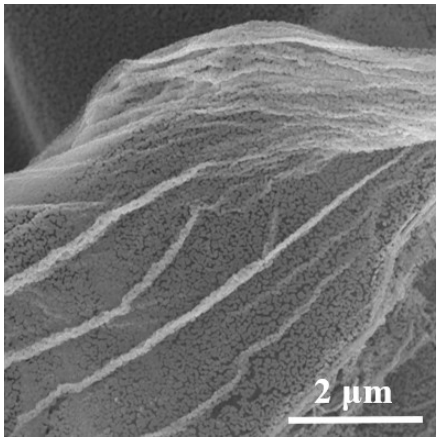

Fig. S4 SEM image of LNO.

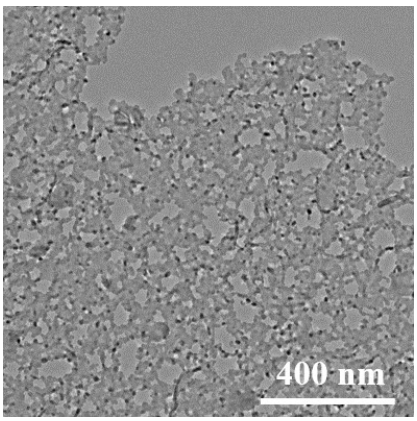

Fig. S5 TEM image of LNO.

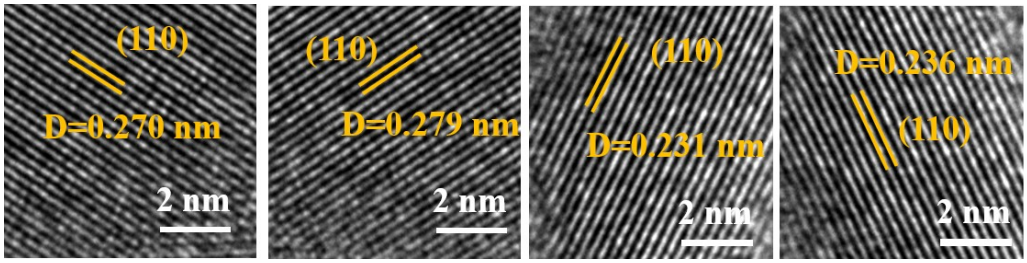

Fig. S6 Lattice spacing of LNO , LNMO-0.4 , LNMO-0.6 , LNMO-0.8 on the (110) diffraction plane.

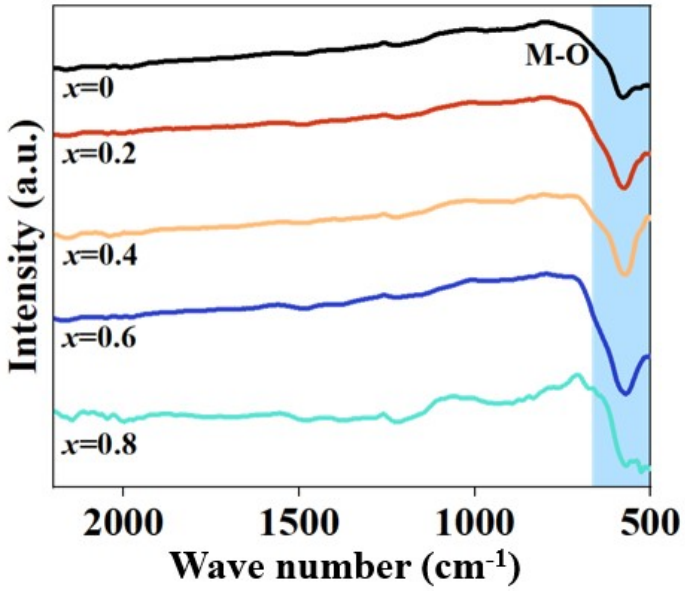

Fig. S7 FTIR spectrums of $LaMn_xNi_{1-x}O_3$ (x=0, 0.2, 0.4, 0.6, 0.8).

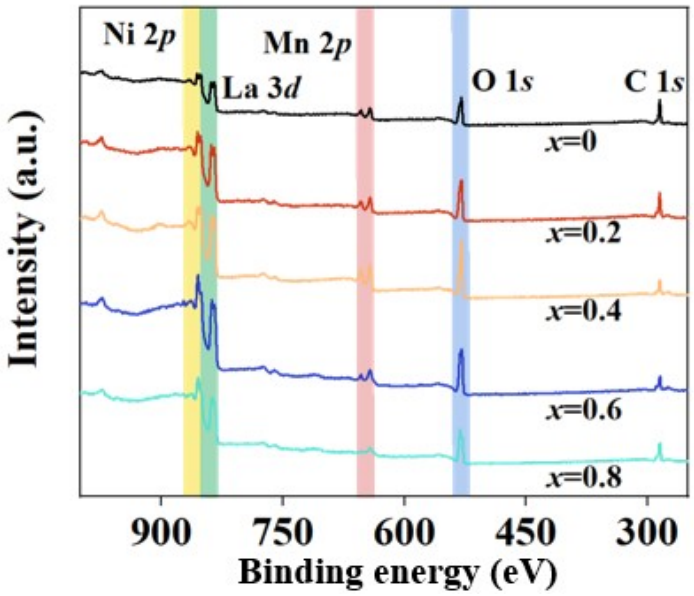

Fig. S8 XPS survey spectrum of $LaMn_xNi_{1-x}O_3$ (x=0, 0.2, 0.4, 0.6, 0.8) catalysts.

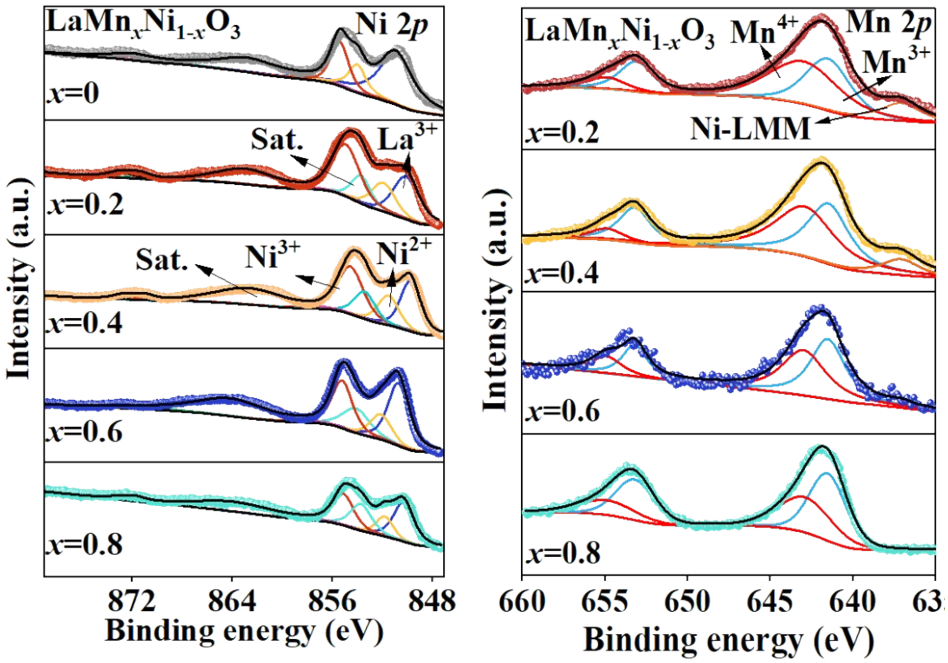

Fig. S9 High-resolution XPS spectra of (A) Ni 2*p* and (B) Mn 2*p* features of $LaMn_xNi_{1-x}O_3$ (x=0, 0.2, 0.4, 0.6, 0.8) catalysts.

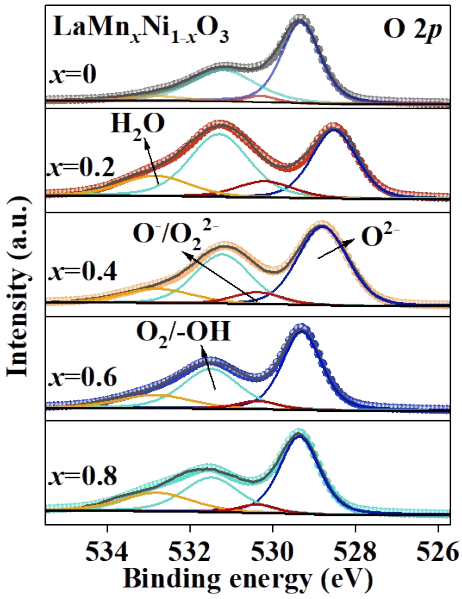

Fig. S10 High-resolution XPS spectra of O 1*s* features of $LaMn_xNi_{1-x}O_3$ (x=0, 0.2, 0.4, 0.6, 0.8) catalysts.

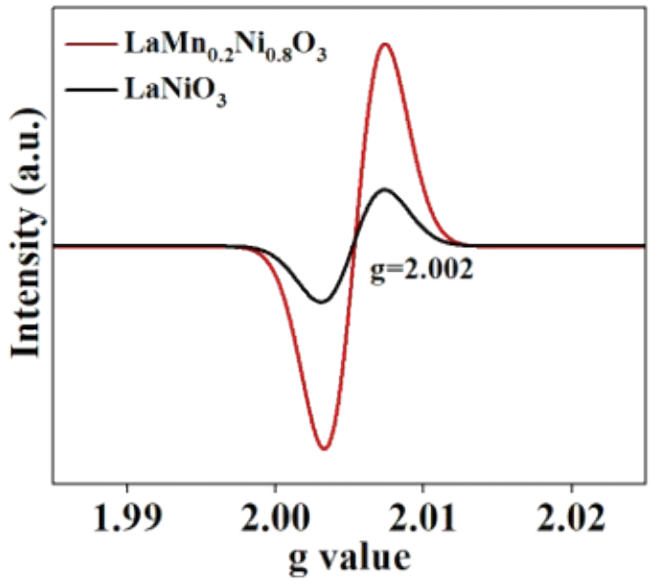

Fig. S11. EPR spectra of LNMO-0.2 and LNO.

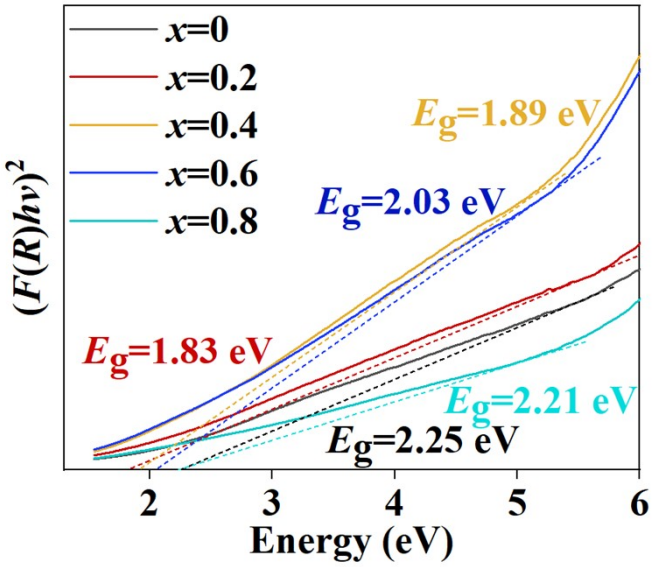

Fig. S12 Bandgap of $LaMn_xNi_{1-x}O_3$ (x=0, 0.2, 0.4, 0.6, 0.8) catalysts.

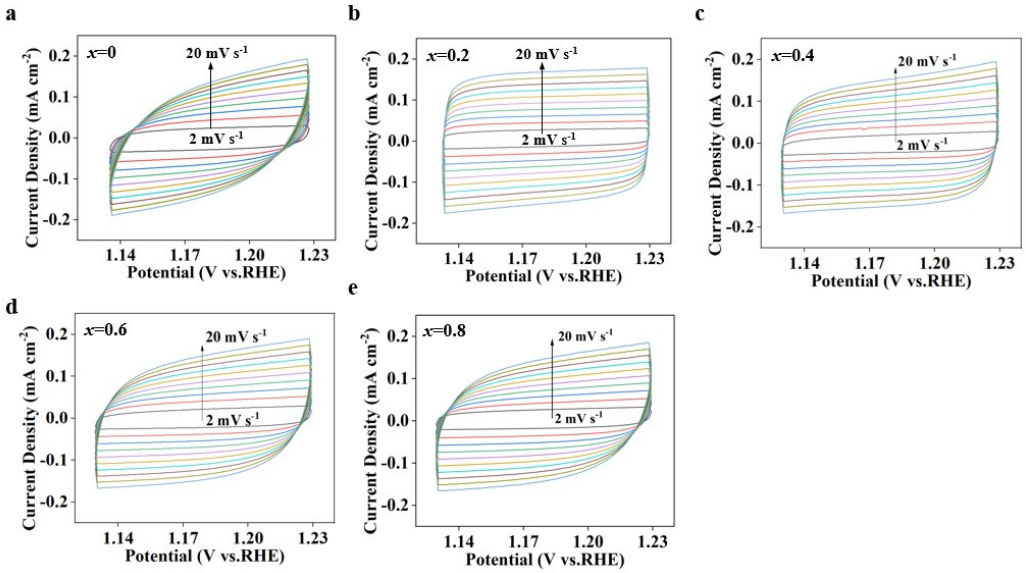

Fig. S13 CV measurements in a non-faradic current region (1.13-1.23 V) at scan rates of 2 to 20 mV $s^{-1}$of (a) $LaNiO_3$, (b) $LaMn_{0.2}Ni_{0.8}O_3$, (c) $LaMn_{0.4}Ni_{0.6}O_3$, (d) $LaMn_{0.6}Ni_{0.4}O_3$ and (e) $LaMn_{0.8}Ni_{0.2}O_3$ in N_2-saturated 1.0 M KOH and 0.33 M urea solution.

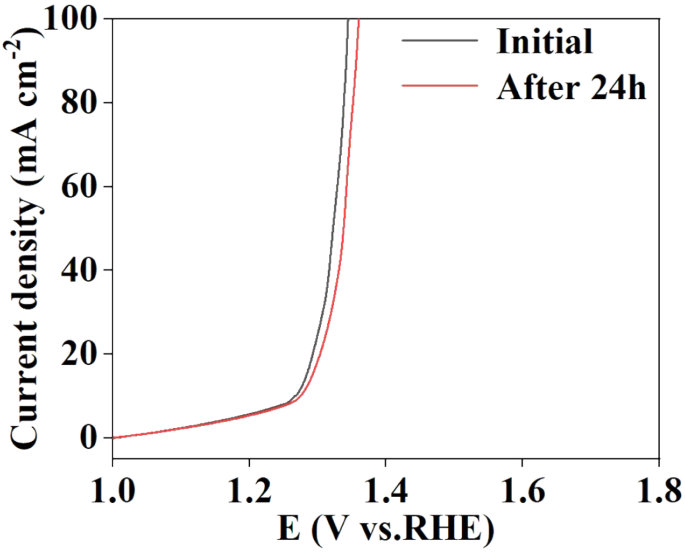

Fig. S14 The durability tests of LNMO-0.2 catalysts.

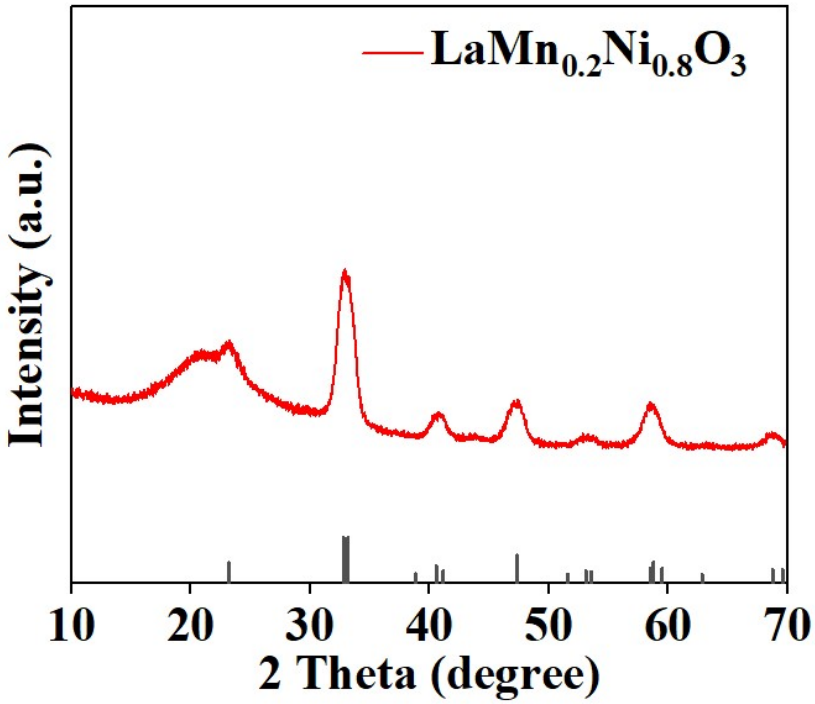

Fig.S15 XRD images of LNMO-0.2 after durability tests.

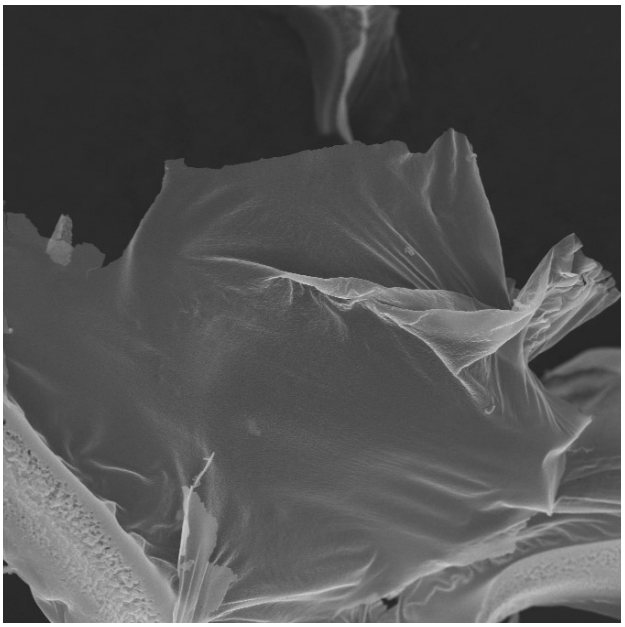

Fig. S16 SEM images of LNMO-0.2 catalysts after durability tests.

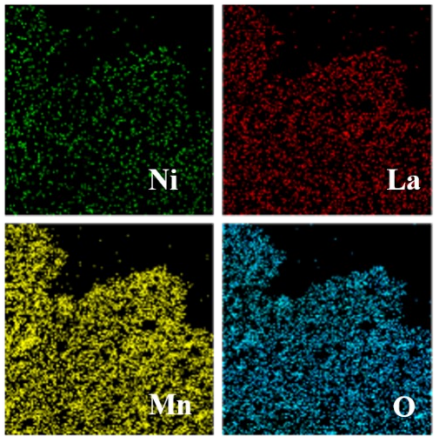

Fig. S17 EDS images of LNMO-0.2 catalysts after durability tests.

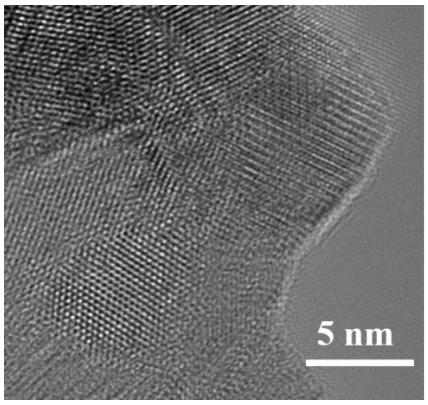

Fig. S18 HRTEM images of LNMO-0.2 catalysts after durability tests.

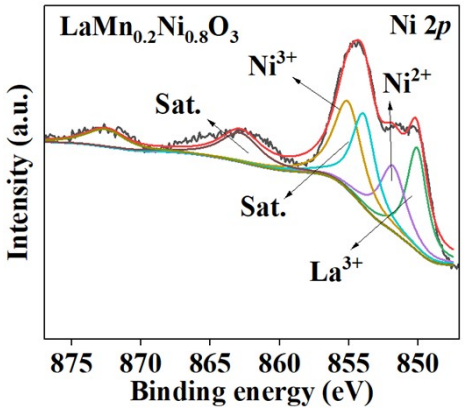

Fig. S19 XPS images of LNMO-0.2 catalysts after durability tests.

2. Table S1 to S2

Table S1. The contents of different LNMO metal elements were measured by LCP-MS

		wavelength	net intensity	concentration (ppm)	concentration (mmol L^{-1})	atomic ratio
x=0	La	408.671	1921	18.72496133	0.134799232	1
	Mn	257.61	35	0	0	0
	Ni	231.604	922	7.839203427	0.142691824	1.05855072
x=0.2	La	408.671	1820	17.74317489	0.127731444	1
	Mn	257.61	183	1.536139822	0.027961335	0.21890722
	Ni	231.604	1105	6.139000498	0.104595105	0.81886732
x=0.4	La	408.671	1539	15.01167002	0.108067598	1
	Mn	257.61	424	2.548949537	0.04342851	0.4018643
	Ni	231.604	510	3.591672067	0.065376826	0.60496233
x=0.6	La	408.671	1502	14.65200568	0.105478408	1
	Mn	257.61	699	3.689318666	0.062857899	0.59593143
	Ni	231.604	280	2.363470228	0.043020682	0.40786245
x=0.8	La	408.671	1326	12.9411699	0.093162263	1
	Mn	257.61	495	4.197243807	0.076399647	0.82007075
	Ni	231.604	254	1.00432257	0.017111454	0.18367366

Table S2. The UOR performance comparison of different catalysts.

Electrocatalysts	Electrolyter	Potenial @10mA cm^{-2} (V)	Tafel slope ($mV\ dec^{-1}$)	Scan rate ($mV\ s^{-1}$)
This work LNMO-0.2	1 M KOH+0.33 M urea	1.27	44.6	10
Co_2GeO_4	1 M KOH+0.33 M urea	1.59	79	10
CuO@CuM	1 M KOH+0.5 M urea	1.44	98.7	5
C@NiO	1 M KOH+0.33 M urea	1.36	87.2	5
Co_2VO_4/NF	1 M KOH+0.5 M urea	1.32	92	5
Co_3O_4/CC	1 M KOH+0.3 M urea	1.67	71	5
MoO_2@CC	1 M KOH+0.33 M urea	1.44	112.2	10
FeNi @NC	1 M KOH+0.33 M urea	1.37	71.6	1
Co_3S_4/CoO_x NTs	1 M KOH+0.5 M urea	1.4	91.3	5
FeNi Oxide-3	1 M KOH+0.33 M urea	1.49	124	1
NiAl-LDHs	1 M KOH+0.33 M urea	1.42	59.8	10
Ni@NCNT-3	1 M KOH+0.5 M urea	1.38	76	2
NF@acid-H_2	1 M KOH+0.33 M urea	1.33	65	10
V-Ni_3N/NF	1 M KOH+0.5 M urea	1.361	45	-
NiCo-BDC-S-6	1 M KOH+0.33 M urea	1.326	46	5
Ni(OH)-S	1 M KOH+0.33 M urea	1.34	53.28	5